

## Converged R-Matrix Calculations of the Photoionization of Fe xvii in Astrophysical Plasmas: from Convergence to Completeness

Lianshui Zhao,<sup>1</sup> Werner Eissner,<sup>2</sup> Sultana N. Nahar,<sup>1</sup> and Anil K. Pradhan<sup>1</sup>

<sup>1</sup>The Ohio State University, Columbus, OH 43210, USA; zhao.1157@osu.edu  
nahar.1@osu.edu pradhan.1@osu.edu

<sup>2</sup>Institut für Theoretische Physik, Universität Stuttgart, 70550 Stuttgart,  
Baden-Württemberg, Germany; we@theo1.physik.uni-stuttgart.de

**Abstract.** We use the relativistic distorted wave (RDW) method to complement (“top-up”) the photoionization cross sections of Fe xvii obtained with the close-coupling Breit–Pauli *R*-Matrix (CC-BPRM) method. There is good agreement between RDW and BPRM for the background cross sections where resonances are not present, and the individual fine-structure levels can be correctly matched spectroscopically. To ensure completeness, we consider a high-energy tail up to 500 Ry above the ionization threshold for each level. The top-up contribution results in a ~20% increment in addition to the 35% enhancement found in BPRM calculations relative to the Opacity Project value for the Rosseland mean opacity at the *Z*-temperature of  $2.11 \times 10^6$  K.

### 1. Introduction

The iron opacity at conditions similar to the solar radiation/convection zone boundary was measured at the Sandia National Laboratory (Bailey et al. 2015), revealing results 30–400% higher than the predictions by theoretical opacity models. To resolve this discrepancy, extensive close-coupling Breit–Pauli *R*-Matrix (BPRM) calculations have been carried out including 60 fine-structure levels within the  $n \leq 3$  complexes in the Fe xviii target ion (60CC-BPRM, Nahar et al. 2011) and 99 *LS* terms within  $n \leq 4$  (99LS-RM). They show strong photon absorption due to core excitation, resulting in an increment of 35% in the Rosseland mean opacity over the Opacity Project (OP) data (Nahar & Pradhan 2016a, hereafter NP16). Whereas the NP16 work demonstrated that in the *R*-Matrix opacity calculations convergence of the close-coupling expansion was a necessary condition for accuracy, completeness of all possible excited configurations at *Z*-plasma temperatures still requires additional contributions in the high-energy range (Blancard et al. 2016; Nahar & Pradhan 2016b; Iglesias & Hansen 2017).

In this paper we address the completeness issue. We adopt the 60CC-BPRM calculation since (i) fine structure is included and is important, and (ii) the 99LS-RM calculation shows background convergence, with additional resonances appearing near the  $n = 4$  Fe xviii thresholds that do not lead to further enhancement of the Fe xvii Rosseland mean opacity, most likely due to the neglect of fine structure. Levels in 60CC-BPRM have also been identified by Nahar et al. (2011).

In the following sections, the specifications of the 60CC-BPRM calculation of Nahar et al. (2011) are summarized, followed by the “top-up” configurations and tran-

sitions calculated with a relativistic distorted wave (RDW) method using the Flexible Atomic Code (FAC), an open-source software package by Gu (2008). To ensure data correspondence from FAC, a comparison of the photoionization cross sections from both FAC and BPRM is carried out. Moreover, to also ensure completeness in energy, the calculation in the high-energy region is extended to 500 Ry using FAC.

## 2. Configurations in 60CC-BPRM

The 60CC-BPRM calculation of the photoionization cross section of Fe xvii is comprehensively detailed in Nahar et al. (2011). The bound and target configurations are summarized as follows:

- Bound configurations:  $2s^22p^6$ ;  $2s^22p^5nl$  with  $n \leq 10$  and  $\ell \leq 7$ ;  $2s2p^6nl$  ( $n \leq 4$ ); and  $2s2p^65s$ .
- Target configurations:  $2s^22p^5$ ;  $2s2p^6$ ; and  $2s^22p^43\ell$ .

In Section 3, all the possible top-up transitions do not include any of those listed above.

## 3. Top-up Configurations and Transitions

To complement the photoionization cross section of 60CC-BPRM, part of the top-up configurations and transitions are taken from Badnell & Seaton (2003), Badnell et al. (2005), and Iglesias & Hansen (2017):

- 454-level L-shell photoionization. The same 454 levels as in 60CC-BPRM but they are considered only as L-shell photoionization excluding any transition that appears in 60CC-BPRM.
- Additional L- and outer-shell photoionization.  $2s2p^65\ell$  ( $\ell > 0$ ) and  $2s2p^6nl$  ( $6 \leq n \leq 10$ ). A type of transition is L-shell photoionization that ionizes an electron in the L-shell leaving the rest intact, the other being “outer-shell” photoionization to any dipole-allowed final state from  $2s2p^6$ ,  $2s^22p^5$ , and  $2s^22p^43\ell$ .
- Two-hole configurations. Each two-hole configuration can be divided into two parts, an inner and an outer, and the two-hole configurations included are formed by combining any inner part with any outer part. Inner part:  $2p^6$ ;  $2s2p^5$ ;  $2s^22p^4$ . Outer part:  $n\ell n'\ell'$  with  $3 \leq n \leq 6$  and  $3 \leq n' \leq 6$ .

The transitions taken into account from the two-hole configurations are: (i) in the outer part, either of the two electrons is ionized leaving the inner part intact; and (ii) an electron is ionized from the L-shell.

Using FAC it is fairly simple to implement the photoionization calculations compared with BPRM, resulting in 51 558 initial levels and more pairs of transitions among them. For each level, an individual energy mesh is created according to the ionization thresholds such that the photoionization cross section is well resolved at all energies. The final photoionization cross section for a level is the sum of all the transitions from the level in the same energy mesh up to 500 Ry above the lowest threshold.

#### 4. Comparison between RDW and BPRM

To top-up the photoionization cross sections of the 454 levels included in 60CC-BPRM with additional L-shell transitions, the energy levels have to be matched between RDW and BPRM. By comparing the total angular momentum  $J$  and parity  $P_i$ , the energy order, and some other factors, they are readily matched up. To ensure correct matching, the RDW calculation is performed on the photoionization cross section from the 454 levels to any possible target state included in 60CC-BPRM, i.e., levels in  $2s^22p^5$ ,  $2s2p^6$ , and  $2s^22p^43\ell$ . Generally the RDW matches well with the background of the BPRM result but excludes all the resonances in BPRM (see Fig. 1).

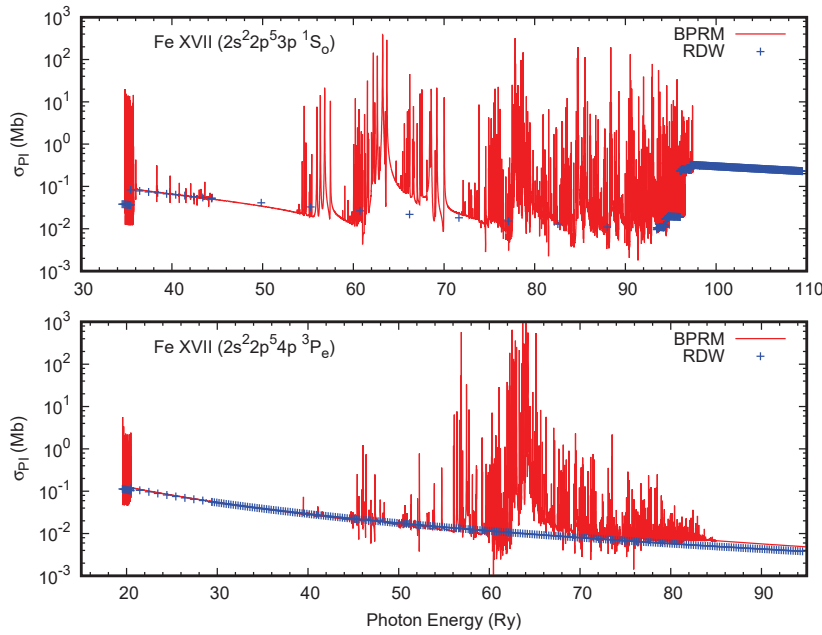


Figure 1. Comparison of the photoionization cross section for two levels of Fe xvii using RDW and BPRM. *Above:*  $2s^22p^53p\ ^1S_0$ . *Below:*  $2s^22p^54p\ ^3P$ .

#### 5. Photoionization Cross Section in the High-Energy Region

Apart from adding more possible configurations and transitions, the energy range where the calculation is performed is extended to 500 Ry above the lowest energy threshold for each level. As the BPRM computation in such a large energy range is intensive and unnecessary, the RDW is used to extend the high-energy “tails” of the photoionization cross section for the 454 levels in 60CC-BPRM. The RDW data are re-scaled by the ratio of the BPRM and RDW photoionization cross sections at the last energy point in BPRM, as the latter should be the more accurate. Kramers’ rule,  $\sigma_\nu = \sigma_1(\nu_1/\nu)^3$ , is also applied for extrapolation in the tail region. It turns out that the opacity contribution from the high-energy regime is equivalent using RDW and Kramers’ rule (see Fig. 2).

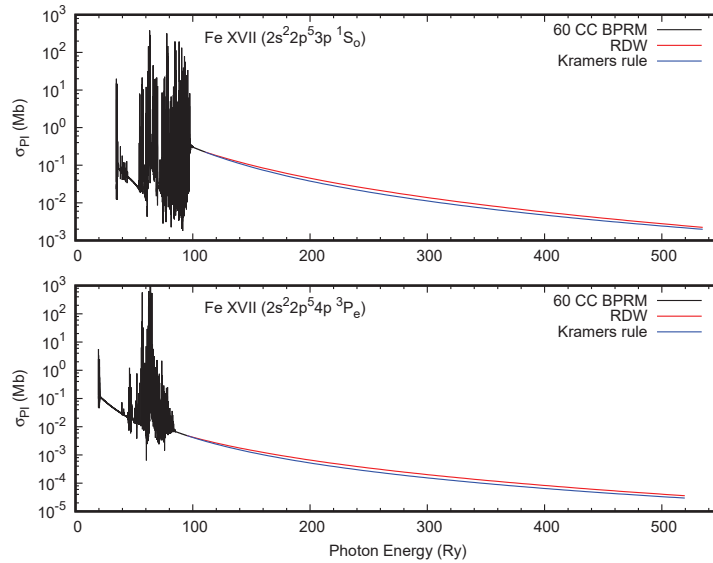


Figure 2. Photoionization cross section of Fe xvii in the high-energy regime using RDW and Kramers' rule. *Above:*  $2s^2 2p^5 3p^1 S_0$ . *Below:*  $2s^2 2p^5 4p^3 P$ .

## 6. Conclusion

Calculation of the photoionization cross section of Fe xvii is completed by including top-up configurations and transitions, and extending its tail to the high-energy bound-free continuum. We find an additional  $\sim 20\%$  enhancement, in addition to the 35% reported in NP16, with the total topped-up result of 1.64 times the OP value for the Rosseland mean opacity at the Z temperature (Pradhan & Nahar 2018). The high-energy top-up is thus close to the 16% estimated in Iglesias & Hansen (2017). However, the actual Fe xvii Rosseland mean opacity might be still larger due to additional fine-structure thresholds from the 218-level BPRM calculation in progress, which includes resonances converging to the  $n = 4$  thresholds of Fe xviii.

**Acknowledgments.** This research was supported by a teaching assistantship from the Dept. of Physics and the Dept. of Astronomy of Ohio State University (OSU) and by the US National Science Foundation and Dept. of Energy. Computations were carried out at the Ohio Supercomputer Center (OSC) and the OSU Dept. of Astronomy.

## References

- Badnell, N.R., Bautista, M. A., Butler, K., et al. 2005, MNRAS, 360, 458  
 Badnell, N. R., & Seaton, M. J. 2003, J. Phys. B – At. Mol. Opt., 36, 4367  
 Bailey, J., Nagayama, T., Loisel, G. P., et al. 2015, Nature, 517, 56  
 Blancard, C., Colgan, J., Cossé, Ph., et al. 2016, Phys. Rev. Lett., 117, 249501  
 Gu, M. F. 2008, Can. J. Phys., 86, 675  
 Iglesias, C., & Hansen, S. 2017, ApJ, 835, 5  
 Nahar, S. N., Pradhan, A. K., Chen, G. X., & Eissner, W. 2011, Phys. Rev. A, 83, 053417  
 Nahar, S. N., & Pradhan, A. K. 2016a, Phys. Rev. Lett., 116, 235003  
 — 2016b, Phys. Rev. Lett., 117, 249502  
 Pradhan, A., & Nahar, S. 2018, this volume